Generation of helical Ince–Gaussian beams with a liquid-crystal display

Joel B. Bentley and Jeffrey A. Davis

Department of Physics, San Diego State University, San Diego, California 92182-1233

Miguel A. Bandres and Julio C. Gutiérrez-Vega

Photonics and Mathematical Optics Group, Tecnológico de Monterrey, Monterrey 64849, México

We generate helical Ince–Gaussian (HIG) beams by using complex amplitude and phase masks encoded onto a liquid-crystal display (LCD). These beams display an intensity pattern consisting of elliptic rings, whose number and ellipticity can be controlled, and a phase exhibiting a number of in-line vortices, each with a unitary topological charge. We show experimental results that display the properties of these elliptic dark hollow beams. We introduce a novel interference technique for generating the object and reference beams by using a single LCD and show the vortex interference patterns. We expect that these HIG beams will be useful in optical trapping applications. © 2006 Optical Society of America

OCIS codes: 050.1970, 140.3300, 100.5090, 230.6120.

Optical elements that contain an angular phase pattern create an optical vortex beam.[1,2] These vortex beams have been generated by a variety of techniques that are discussed elsewhere[3] and have been used for such applications as optical trapping[4] and image processing.[5] Although the charge of the vortex can be controlled, these vortex beams always show a circular doughnut-shaped intensity pattern. In actuality these angular phase patterns are phase-only approximations of circularly symmetric Laguerre–Gaussian (LG) beams.

Linearly polarized Ince–Gaussian (IG) beams[6,7] form the third complete family of eigenmodes of stable resonators, joining the well-known Hermite–Gaussian (HG) and LG beams. The even and odd IG beams are exact solutions of the scalar paraxial wave equation in elliptic coordinates and are written (at the waist plane $z=0$) as

$$\mathrm{IG}^{e}_{p,m,\epsilon}(\mathbf{r}) = AC^{m}_{p}(i\xi,\epsilon)C^{m}_{p}(\eta,\epsilon)\exp(-r^2/{w_0}^2), \quad (1a)$$

$$\mathrm{IG}^{o}_{p,m,\epsilon}(\mathbf{r}) = BS^{m}_{p}(i\xi,\epsilon)S^{m}_{p}(\eta,\epsilon)\exp(-r^2/{w_0}^2), \quad (1b)$$

where the superindices e and o refer to even and odd beams, respectively, and A and B are normalization constants such that the integral of the intensities is unitary. The transverse distributions are described by the even and odd Ince polynomials, C^{m}_{p} and S^{m}_{p}, of order p and degree m, while ξ and η are the radial and angular elliptic coordinates defined by $x=w_0(\epsilon/2)^{1/2}\cosh\xi\cos\eta$, $y=w_0(\epsilon/2)^{1/2}\sinh\xi\sin\eta$. The ellipticity parameter ϵ controls the transition between the LG beams (where $\epsilon=0$) and the HG beams (where $\epsilon=\infty$).

The transverse shape of the beams is described by the three parameters p, m, and ϵ, where $0\leqslant m\leqslant p$ for even beams, $1\leqslant m\leqslant p$ for odd beams, and p and m always have the same parity; i.e., $(-1)^{p-m}=1$. The degree m controls the number of hyperbolic nodal lines, while the number of elliptic nodal lines is given by $(p-m)/2$, not including the interfocal nodal line for the case of odd beams. For a given light wavelength, the waist w_0 scales the physical size of the beam. The propagation characteristics of these beams are discussed elsewhere.[6,7]

Many groups have successfully generated the phase-only approximations for the LG beams by using spatial light modulators and holograms.[4] The even IG beams have also been demonstrated experimentally in a stable solid-state laser resonator.[8]

In this work we generate for the first time (to our knowledge) the helical Ince–Gaussian (HIG) beams. These HIG beams display elliptical intensity rings containing a number of in-line vortices rather than a circular intensity ring containing a single vortex. The number of rings, number of vortices, and ellipticity of the rings can all be controlled through the choice of the HIG beam parameters.

HIG beams can be constructed[7] by forming a linear combination of the even and odd IG beams as

$$\begin{aligned}\mathrm{HIG}^{\pm}_{p,m,\epsilon}(\xi,\eta) &= \mathrm{IG}^{e}_{p,m,\epsilon}(\xi,\eta,\epsilon) \pm i\mathrm{IG}^{o}_{p,m,\epsilon}(\xi,\eta,\epsilon)\\ &= M(x,y)\exp[i\phi(x,y)], \end{aligned} \quad (2)$$

where $M(x,y)$ and $\phi(x,y)$ are the amplitude and the phase of the HIG beam in Cartesian coordinates.

The $\mathrm{LG}_{n,l}$ beams are characterized by an angular phase dependence of $\exp(\pm il\phi)$ and $n+1$ intensity rings surrounding a vortex having a topological charge of l. By contrast, the HIG beams are characterized by $N=[1+(p-m)/2]$ elliptic rings and have m physically separated vortices, each with a unitary topological charge. The ellipticity of the rings is controlled by the parameter ϵ. As the ellipticity approaches zero, these separated vortices spatially collapse to a single vortex with the total charge of m.

To encode these patterns, we multiply the HIG pattern from Eq. (2) by a linear phase grating having a period d, as

$$M(x,y)\exp\{i[\phi(x,y)+2\pi x/d]\}. \quad (3)$$

The total phase is the sum of the HIG phase term with the grating phase. Amplitude information can be encoded onto a phase-only recording medium by

0146-9592/06/050649-3/$15.00

spatially modulating the phase pattern with the amplitude portion of the HIG pattern,[9,10] as

$$\exp\{iM(x,y)[\phi(x,y)+2\pi x/d]\}, \tag{4}$$

where the phase is in the range $[-\pi,\pi]$ and the amplitude is defined in the range $[0\leqslant M(x,y)\leqslant 1]$. As the phase depth increases, the intensity diffracted into the first order increases while the zero-order intensity decreases. The idea is fundamentally different from the usual concept of amplitude operation. Normally an amplitude filter blocks the light from going in a certain direction. Here we do not block the light but simply direct it in a different direction.

In our experiments, linearly polarized light from an argon laser is spatially filtered, expanded, and collimated, effectively forming a plane wave. The optical elements are encoded onto a parallel-aligned nematic liquid-crystal display (LCD, manufactured by Seiko Epson with 640×480 pixels on a 1.3 in. display.[11] Each pixel acts as an electrically controllable phase plate, where the total phase shift exceeds 2π rad as a function of gray level at the argon laser wavelength of 514.5 nm.

We used a value of $d=8$ pixels and added a focusing lens to the system to separate the Fourier transform of the first-order HIG beam from the zero-order intensity. The output was then recorded with a CCD camera.

Figures 1(a) and 1(b) show the theoretical magnitude and phase patterns for the $\mathrm{HIG}^{+}_{6,6,3}$ beam. The patterns are written as 512×512 arrays by using a waist size w_0 of 56 pixels. Figure 1(c) shows the sum of the linear phase shift and the HIG phase. Finally, Fig. 1(d) shows the amplitude-modulated phase pattern by using the recipe of Eq. (4). When we send these patterns to the LCD, we overfill the display in one dimension and underfill it in the other dimension.

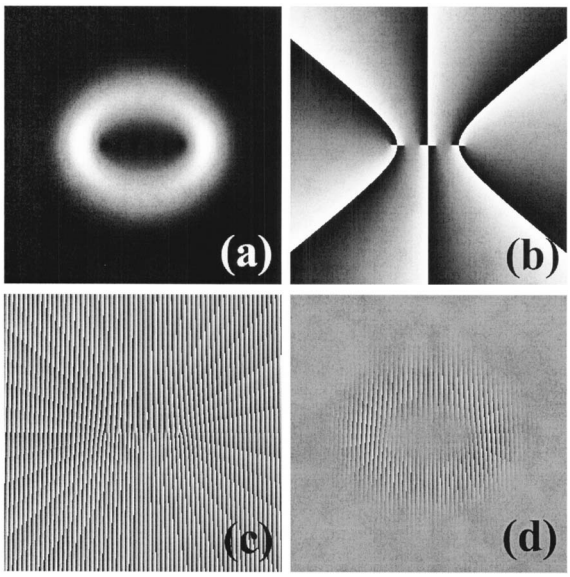

Fig. 1. Computer masks for the $\mathrm{HIG}^{+}_{6,6,3}$ beam, showing (a) magnitude, (b) phase, (c) linear phase added to HIG phase, and (d) amplitude-modulated phase mask.

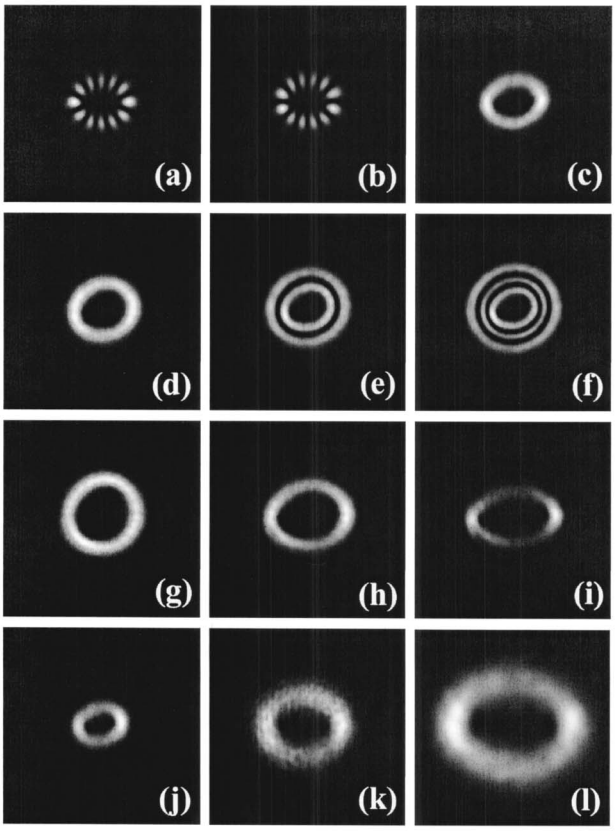

Fig. 2. Experimental intensity results, showing (a) even $\mathrm{IG}_{6,6,3}$ beam, (b) odd $\mathrm{IG}_{6,6,3}$ beam, (c) $\mathrm{HIG}^{+}_{6,6,3}$ beam, (d) one intensity ring for the $\mathrm{HIG}^{+}_{8,8,2}$ beam, (e) two intensity rings for the $\mathrm{HIG}^{+}_{10,8,2}$ beam, (f) three intensity rings for the $\mathrm{HIG}^{+}_{12,8,2}$ beam, (g) zero-ellipticity $\mathrm{HIG}^{+}_{12,12,0}$ beam, (h) higher ellipticity $\mathrm{HIG}^{+}_{12,12,6}$ beam, (i) high ellipticity $\mathrm{HIG}^{+}_{12,12,12}$ beam; intensity for the $\mathrm{HIG}^{+}_{4,4,2}$ beam at (j) the focal plane, (k) 0.8 m, and (l) 1.0 m. Photographs show 600×600 camera pixels with sizes of 6.7 μm square.

Experimental results are shown in Fig. 2. The even and odd $\mathrm{IG}_{6,6,3}$ beams are shown in Figs. 2(a) and 2(b), respectively. Note that the bright spots for the odd and the even beams are at alternate points in the ellipse. Figure 2(c) shows the $\mathrm{HIG}^{+}_{6,6,3}$ beam, and we see a single elliptical intensity ring as expected. The light intensity increases near the foci and decreases elsewhere, consistent with the theoretical magnitude shown in Fig. 1(a). Results using phase-only modulation would be acceptable for many applications, but the amplitude and phase results were superior.

The number of rings is controlled by the parameter N. To show this, we fixed the value of $m=8$ and changed the value for p. Experimental results are shown for in Fig. 2(d) for the $\mathrm{HIG}^{+}_{8,8,2}$ beam, in Fig. 2(e) for the $\mathrm{HIG}^{+}_{10,8,2}$ beam, and in Fig. 2(f) for the $\mathrm{HIG}^{+}_{12,8,2}$ beam. The number of rings increases from 1 to 3. We also see that the overall diameter of the pattern increases as the parameter p increases.

The ellipticity of the beam depends on the ellipticity parameter ϵ as shown in Fig. 2(g) for the $\mathrm{HIG}^{+}_{12,12,0}$ beam, in Fig. 2(h) for the $\mathrm{HIG}^{+}_{12,12,6}$ beam, and in Fig. 2(i) for the $\mathrm{HIG}^{+}_{12,12,12}$ beam. The change

in ellipticity was more dramatic for larger values of p and m than for smaller values. As the ellipticity parameter decreases to zero, the HIG beams tend toward the LG beams, as discussed above.

There are two tests to confirm that these are actual solutions for the paraxial wave equation. First, we performed measurements at different z planes to corroborate that the beams are structurally stable; i.e., they do not change shape on propagation except by the well-known scale factor $w_0/w(z)$ of the Gaussian beams.[6] This behavior can be appreciated in Figs. 2(j)–2(l), where we show the measured intensity distributions for the $\mathrm{HIG}^{+}_{4,4,2}$ beam at the focal plane of the lens and at 0.8 and 1.0 m from this plane. Unlike the well-known LG and Bessel beams, the HIG beams are dark elliptic hollow beams that exhibit an azimuthally asymmetric angular momentum density and intensity profile. This feature might be useful to control the rotational motion of microparticles along the elliptic rings of the HIG beams with the advantage that the ellipticity can be adjusted dynamically.

Finally, the theory predicts that there are m vortices within the central dark ellipse. Their existence can be shown by using a novel interference experiment. We use the same approach as in Eq. (4) with two changes. First, we change the relative sizes of the two beams by decreasing the range for the parameter $M(x,y)$. Now the phase depth modulation creates both the on-axis HIG beam along with an off-axis plane wave. For example, if $M(x,y)$ is in the range $[0 \leqslant M(x,y) \leqslant 0.5]$, then the zero- and first-order intensities will be more comparable. Second, we increase the period d of the grating so that the zero- and first-order beams overlap to display interference fringes. By controlling the phase depth, we can vary the intensities of these two beams and the contrast of the interference fringes. The period of the interference fringes is controlled by the parameter d. Now we place the detector in a region where the two beams overlap. By adjusting the range for $M(x,y)$, we can change the contrast of the interference fringes. These interference lines will split at the locations of the vortices.

Experimental results in Fig. 3 validate this approach for the $\mathrm{HIG}^{+}_{3,3,\epsilon}$ beam, where we used a value of $d=19$ pixels Figure 3(a) shows the case where $\epsilon=3$, and three dislocations are clearly seen in the interference fringes. As we decrease the ellipticity parameter to $\epsilon=0.5$, the vortices become closer as shown in Fig. 3(b). Finally, as the ellipticity parameter decreases to zero in Fig. 3(c), the m individual vortices collapse to a single vortex with a total charge of m. Computer simulations agree with experimental results in all cases and, consequently, are not shown.

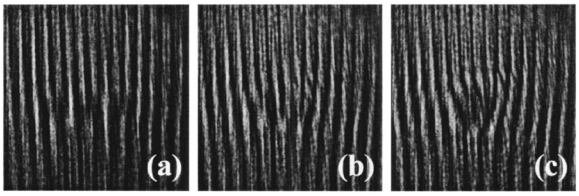

Fig. 3. Experimental interference pattern, showing positions of vortices as the ellipticity parameter decreases: (a) $\epsilon=3$, (b) $\epsilon=0.5$, (c) $\epsilon=0$.

In conclusion, we have experimentally demonstrated the HIG beams by passing light through an appropriate amplitude and phase mask encoded onto a LCD. Although the phase-only pattern works well, these more complicated beams are improved by encoding both amplitude and phase information. We examined the vortices by using a new self-interference approach, again using a single LCD. The properties of these beams agree with theoretical predictions, and we look forward to the implementation of these beams in optical trapping experiments.

We thank Tomio Sonehara of Seiko Epson Corporation for the use of the LCD. J. C. Gutiérrez-Vega acknowledges support from the Consejo Nacional de Ciencia y Tecnología of Mexico (grant 42808). J. Davis's e-mail address is jdavis@sciences.sdsu.edu.

References

1. M. Mansuripur and E. M. Wright, Opt. Photon. News **10(2)**, 40.
2. J. F. Nye and M. V. Berry, Proc. R. Soc. London Ser. A **336**, 165 (1974).
3. K. Crabtree, J. A. Davis, and I. Moreno, Appl. Opt. **43**, 1360 (2004).
4. H. He, N. R. Heckenberg, and H. Rubinsztein-Dunlop, J. Mod. Opt. **42**, 217 (1995).
5. J. A. Davis, D. E. McNamara, D. M. Cottrell, and J. Campos, Opt. Lett. **25**, 99 (2000).
6. M. A. Bandres and J. C. Gutiérrez-Vega, Opt. Lett. **29**, 144 (2004).
7. M. A. Bandres and J. C. Gutiérrez-Vega, J. Opt. Soc. Am. A **21**, 873 (2004).
8. U. T. Schwarz, M. A. Bandres, and J. C. Gutiérrez-Vega, Opt. Lett. **29**, 1870 (2004).
9. J. A. Davis, D. M. Cottrell, J. Campos, M. J. Yzuel, and I. Moreno, Appl. Opt. **38**, 5004 (1999).
10. J. A. Davis, D. A. Smith, D. E. McNamara, D. M. Cottrell, and J. Campos, Appl. Opt. **40**, 5943 (2001).
11. J. A. Davis, P. Tsai, D. M. Cottrell, T. Sonehara, and J. Amako, Opt. Eng. **38**, 1051 (1999).